Resource adequacy in grids with deepening penetrations of integrated renewable resources

Mariola Ndrio and George Gross
Department of Electrical and Computer Engineering
University of Illinois at Urbana-Champaign, Urbana IL 61801, USA
Email: {ndrio2, gross}@illinois.edu

***Abstract*—As the penetrations of renewable energy resources deepen in electric power grids around the world, their impacts on the grid's resource adequacy become more significant. The marked intermittent and time-varying nature of renewable resources (*RR*s) cannot be appropriately represented in the widely-used time-invariant resource adequacy evaluation approach. This paper reports on the development of a resource adequacy evaluation framework with the capability to represent the uncertain and time-varying nature of demand and supply resources, including those of renewable technologies. The deployment of stochastic-process-based models to effectively represent all grid-integrated resources captures the intermittent, time-varying and uncertain nature of the *RR*s. The framework uses Monte Carlo simulation as the primary tool for the evaluation of the widely-used resource adequacy metrics as well as the sensitivity measures introduced to quantify the impacts of deepening *RR* penetrations on these metrics. We present representative results from our extensive application studies on a realistic large-scale system with total installed capacity of 40,000 *MW* and projected summer peak demand equal to 36,800 *MW*. The results quantify the behavior of the resource adequacy metrics as the *RR* penetrations deepen. Specifically, the results indicate the distinct character of deepening solar and wind penetrations and their common diminishing returns feature. When the planned retirement of fossil-fired generation units is also considered, it becomes clear that additional resources are needed to maintain the grid's ability to meet the industry-wide "1 day in 10 years" resource adequacy criterion. The proposed framework, provides a useful assessment mechanism to prepare large-grid operators in the transition to the greener electricity future. In addition, the framework is sufficiently general to allow the representation of distributed energy resource aggregations that are starting to play an increasingly significant role in bulk power systems. The study results presented effectively illustrate the challenges faced by the electric power industry in the resource adequacy area.**

***Index Terms*—resource adequacy, renewable resources, Monte Carlo simulations, reliability, resource adequacy metrics, sensitivity of resource adequacy metrics**

I. Introduction

The growing worldwide concern over the climate change manifests itself in the increased implementation of *RR* integration into electricity grids to bring about the cost-effective reduction in greenhouse gas emissions and alleviate each nation's dependence on foreign fuels [1]–[3]. However, as the penetrations of *RR*s deepen in electric grids around the world, there are rising concerns on the impacts that such resources may have on the grids' resource adequacy. Resource adequacy is generally defined as the ability of the bulk power system to supply the aggregate power and energy requirements of the consumers at all times taking into account scheduled and unscheduled outages of system components [4]. In this context, all supply resources are considered, including conventional fossil-fired and nuclear units, *RR*s as well as demand response resources (*DRR*s). The latter refer to loads capable to adjust their consumption in response to price signals that provide incentives to curtail consumption and allow loads to actively participate in ensuring supply-demand equilibrium [5]. In resource adequacy studies, we are interested in situations where the so-called firm load obligations of the system exceed the instantaneous available generation capacity and consequently result in the involuntary curtailment of firm electricity supply to load customers [6]. We refer, typically, to such situations as loss of load ($\ell.o.\ell.$) events. In general, $\ell.o.\ell.$ events are caused by one or more component outages, but not every component outage results in a $\ell.o.\ell.$ event. Resource adequacy assessment involves the investigation of $\ell.o.\ell.$ events in the study system, to evaluate the probability of such events over a specified period of time and to quantify the ramifications of such losses.

The conventional quantification techniques adopted for resource adequacy studies are based on probabilistic methodologies that involve the evaluation of various resource adequacy metrics, such as the loss of load probability (*LOLP*), the loss of load expectation (*LOLE*), the loss of load hours (*LOLH*) and the expected unserved energy (*EUE*). The principal use of such metrics is in planning studies to allow for the side-by-side comparison of different alternative resource mixes to meet the forecasted electricity demand over a specified period of time. Appropriate criteria are set to determine the boundary between the acceptable or adequate outcomes and those that are not. For example, the utility industry and practitioners have adopted for years the widely-used "1 day in 10 years" criterion, which requires that electric power systems maintain sufficient generation capacity and *DRR*s so that the event that the system peak load exceeds the system available supply occurs once in a 10-year period. Although it is not set as the *de jure* resource adequacy standard, the "1 day in 10 years" is so well entrenched in the industry that it has become a *de facto* criterion for reliability or resource adequacy in North America.

The continual changes in the resource mix brought about by the deeper penetrations of intermittent generation, introduce new challenges to resource adequacy studies due to the distinct time-varying, intermittent and uncertain nature of *RR*s. While

unscheduled or *forced* outages [7] in conventional units are, typically, due to various failures, renewable technology units — although characterized by high availability — can only generate electricity when the fuel is available, e.g., the wind blows within the acceptable ranges. Hence, the static, multi-state representation of *RR*s [8] in the conventional time-abstracted framework and its various extensions [9], is unable to appropriately represent their uncertain and time-varying output as well as their temporal correlations. Therefore, there is an acute need for resource adequacy assessment tools that can explicitly account for the *RR* intermittent and stochastic nature.

As *RR* penetrations deepen, the assessment of the impacts of the changes in penetrations on the grid's resource adequacy, becomes also of acute interest. The North American Electric Reliability Corporation (*NERC*) has repeatedly called for adequacy studies that "provide ongoing evaluation of the potential impacts of the new variable generation on the grid" [10]. Significant contribution in this direction is the study presented in [11]. With data of up to 10 years of wind outputs for the Irish power system, the authors evaluate the effective load carrying capability (*ELCC*) [12] for wind and analyze the effects of the number of wind farms, the data time period and data time resolution on the wind capacity contributions. Similar studies on solar resources [13] have a commonality with those on wind since they fail to assess the impacts of deepening *RR* penetrations on the widely-adopted resource adequacy metrics. Such studies are critically important in order to allow meaningful comparisons among the metrics, shed light on the requirements for additional metrics and contribute to the *NERC*'s vision for "more widely-adopted energy-related reliability metrics and targets as the share of variable generation increases in the power system" [10]. This paper directly addresses this issue and presents a resource adequacy evaluation framework that serves as the vehicle to get to the *NERC*'s vision.

The paper consists of four additional sections. We focus on the construction of the resource adequacy evaluation framework in section II and discuss the key aspects of its application in section III. In section IV, we present representative results from the extensive simulation studies performed with the proposed framework and section V concludes the paper.

II. Brief Review of the Resource Adequacy Framework

The resource adequacy framework is a stochastic simulation-based approach that provides the appropriate representation of the uncertain and time-varying nature of the system loads and the generation resources — particularly the *RR*s. The proposed framework is constructed under the following fundamental assumptions:

- $A\,1$ The only sources of uncertainty considered are in the system loads and supply resources.
- $A\,2$ The uncertainty in the loads is independent of that in the supply resources.
- $A\,3$ The failures/repairs of the system supply resources occur independently of each other.

At the outset, we define the smallest indecomposable unit of time, i.e., the resolution of time used, which is typically study dependent. The framework can be used to perform a study over a given period $\mathscr{T}$, usually specified as a set of hours or days. Hourly (daily) time resolution implies that the smallest indecomposable unit of time is one hour (day) and no phenomena of shorter duration can be represented. Without any loss of generality, throughout this paper we adopt an hourly time resolution for the study period. As such, we denote by $\mathscr{T}_h$ the study period represented by the set that consists of H non-overlapping hourly time units and is defined as $\mathscr{T}_h = \{h : h = 1, 2, \ldots, H\}$.

In the proposed framework, the system loads and the supply/demand resources, are modeled as discrete time random processes (*r.p.*s), whose distribution have no analytical characterization. More specifically, for the study period $\mathscr{T}_h$, we represent the system load as a discrete-time random process (*r.p.*) denoted by $\left\{\underset{\sim}{L}[h] \;:\; h = 1, 2, \ldots, H\right\}$. The *r.p.* is a collection of time-indexed random variables (*r.v.*s) where each $\underset{\sim}{L}[h]$ represents the *r.v.* of the system load in hour h. The sample space $\Omega_{\left\{\underset{\sim}{L}[h] \;:\; h=1,2,\ldots,H\right\}}$ of the system load *r.p.* is assembled using historical data where each set of H hourly loads $\{\ell[h] \;:\; h = 1, 2, \ldots, H\}$ represents a sample path (*s.p.*) of $\left\{\underset{\sim}{L}[h] \;:\; h = 1, 2, \ldots, H\right\}$. Such a representation explicitly considers the time-correlations among hourly loads, since every historical *s.p.* has the time-correlation of the hourly loads embedded in it. Each *s.p.* is assumed to be equiprobable with probability one over the total number of *s.p.*s making up the sample space.

We next consider the representation of the conventional generation resources in the supply system that consists of G such resources and we denote them by the set $\mathscr{G} = \{g_{_k} : k = 1, 2, \ldots, G\}$. Each $g_{_k} \in \mathscr{G}$ denotes a generation plant that may consist of a single or a block of units and from now on we will use the term unit to refer to any such generation plant. For each conventional generation unit $g_{_k} \in \mathscr{G}$, we denote by $\underset{\sim}{A}_k[h]$ the unit's available capacity *r.v.* in hour h. Assumption $A\,3$ implies that for each hour h the state of unit k is independent of the state of any other unit k', $k' \neq k$. Hence, $\underset{\sim}{A}_k[h]$ and $\underset{\sim}{A}_{k'}[h]$ are statistically independent *r.v.*s. In order to capture the variation of the availability of each conventional unit, we deploy a discrete Markov process with the appropriate number of states, where the transition times between states are assumed statistically independent and exponentially distributed *r.v.*s. As such, we denote the availability of each unit $g_{_k} \in \mathscr{G}$ by the discrete-time *r.p.* $\left\{\underset{\sim}{A}_k[h] : h = 1, 2, \ldots, H\right\}$. By sampling the transition-time exponential distribution, we can determine the time period that the unit $g_{_k}$ spends at each of the capacity states. The statistical independence assumption allows for the construction of individual *s.p.*s for each $g_{_k} \in \mathscr{G}$. The collection of

hourly realizations $\{a_k[h] : h = 1, 2, \ldots, H\}$ constitutes a *s.p.* of resource g_k's available capacity and it essentially represents a sequence of states through which the unit passes over each hour of the period $\mathscr{T}_h$. The methodology for simulating the available capacity of conventional generation resources is well documented in the literature and interested readers can refer to [14] for more details. The total available capacity in the system can be represented as a discrete-time *r.p.* with *s.p.*s constructed by summing the individual *s.p.*s of the availability of each unit g_k.

To incorporate the *RR* stochastic and time-varying nature we take advantage of the net load concept, i.e., the net difference between the total system load and the total *RR* power outputs (including the net scheduled interchanges) [15]. In other words, the net load is the load that has to be met by the conventional generation resources. Clearly the net load, by definition, incorporates the intermittent and time-varying effect of *RR*s. In this regard, we represent the *RR*s as discrete-time *r.p.*s, similar to those of load and conventional supply resource representations. As such the net load, just as the *RR*s and the system load, is itself a discrete-time *r.p.*, whose *s.p.*s are constructed from the *s.p.*s of the *RR* and load *r.p.*s.

We consider the system with G conventional resources and integrated groups of *RR*s from different technology types. We define a technology type group of *RR*s to be the set of all the integrated generation plants of the same renewable generation technology. For example, the set of all solar farms integrated into the grid constitutes a distinct *RR* technology type group. Similarly, the set of all the integrated wind farms constitutes another group. We assume there are Q technology type groups of *RR*s integrated into the system. For each group q, we denote the aggregate generation output of the group by the *r.p.* $\left\{\underset{\sim}{R}^q[h] : h = 1, 2, \ldots, H\right\}$. In order to construct a *s.p.* for the $\underset{\sim}{R}^q[h]$ *r.p.*, we make use of historical data[1] from multiple units in the group q. For all the Q groups of *RR*s integrated into the grid, we define their aggregate generation output by the *r.p.* $\left\{\underset{\sim}{R}[h] : h = 1, 2, \ldots, H\right\}$ with *s.p.* $\{r[h] : h = 1, 2, \ldots, H\}$, derived by summing the *s.p.*s of the $\underset{\sim}{R}^q[h]$ *r.p.* for each *RR* group q. We further define the vector of *RR* installed capacity $\underline{\boldsymbol{\kappa}} \in \mathbb{R}^Q$ as

$$\underline{\boldsymbol{\kappa}} = \left[\kappa^1 \;\; \kappa^2 \;\; \ldots \kappa^Q\right]^\dagger \;, \tag{1}$$

where κ^q denotes the total installed capacity in MW of the *RR* technology group q. At a specified level of *RR* installed capacity $\underline{\boldsymbol{\kappa}}$, we incorporate the *RR*s in the resource adequacy framework via the modification of the system load: we subtract each aggregate *RR* generation output *s.p.* from the system load *s.p.* that corresponds to the same time-period. The generated *s.p.* represents a *s.p.* for the net load. In mathematical terms,

[1]We assume that the historical data for the construction of the sample space of the *RR r.p.*s correspond to the same time period as the load historical data. Such practice aims to ensure that the weather correlation between demand and *RR* generation output is taken into consideration.

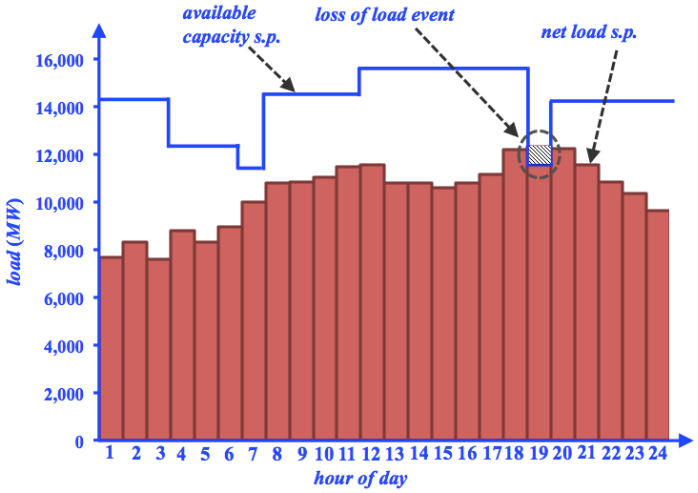

Fig. 1. Determination of loss of load events via comparison of the net load and availability *s.p.*s.

we represent the net load at a level of $\underline{\boldsymbol{\kappa}}$ *RR* installed capacity, by the discrete-time *r.p.*

$$\left\{\underset{\sim}{L}[h]\Big|_{\underline{\boldsymbol{\kappa}}} = \underset{\sim}{L}[h] - \underset{\sim}{R}[h] : h = 1, 2, \ldots, H\right\}, \tag{2}$$

with a *s.p.* given by the set

$$\left\{\ell[h]\Big|_{\underline{\boldsymbol{\kappa}}} = \ell[h] - r[h] : h = 1, 2, \ldots, H\right\} \;. \tag{3}$$

Each *s.p.* has an associated probability equal to one over the total number of *s.p.*s in the sample space of $\underset{\sim}{L}[h]\Big|_{\underline{\boldsymbol{\kappa}}}$.

The evaluation framework makes use of Monte Carlo simulation techniques [16] for the efficient sampling of the load and *RR r.p.*s as well as the conventional unit availabilities in order to simulate the behavior of the system and generate the realizations of the outputs of the resources and loads. From the obtained realizations we can approximate the resource adequacy metrics of the sytem for the entire study period. More specifically, multiple runs of the simulation procedure are performed for a given study period $\mathscr{T}_h$. At every simulation run, *s.p.*s of the system load, *RR* output and generation unit availability are randomly sampled. The *s.p.*s of the units are combined to produce the *s.p.* of the total available capacity in the system while the *s.p.* of the *RR* output is subtracted from the load *s.p.* to derive the *s.p.* of the net load. The realization of the net load is superimposed on the realization of the total available capacity as illustrated in Fig. 1. By observing the realized behavior of the system, we count the $\ell.o.\ell.$ event occurrences and record their duration for the entire study period $\mathscr{T}_h$. Fig. 1 shows a single-day net load *s.p.* that is compared with the daily *s.p.* of the total available capacity. For the particular realization of the system net load and supply availability, we can readily register the occurrence of the $\ell.o.\ell.$ events — namely the single event at 7 PM — and measure its magnitude. The example in Fig. 1 represents a single simulation run of the system, for a day study period.

In order to produce estimates of the resource adequacy metrics with good fidelity we need to repeat the experiment multiple times as detailed in [17].

The quantification of resource adequacy entails the evaluation of the probability of a $\ell.o.\ell.$ event over the specified period $\mathscr{T}_h$. The probability of a $\ell.o.\ell.$ event or *LOLP*, is defined as the probability of the event that load exceeds the total available generation capacity in the system [18]. Under hourly time resolution of the system load representation, the *LOLP* for the entire period $\mathscr{T}_h$ is often referred to as *LOLH* to denote the expected number of hours with an $\ell.o.\ell.$ event in the period $\mathscr{T}_h$. The daily counterpart of the *LOLH* metric is the *LOLE*. The *LOLE* index for a specified period, is defined as the expected number of days with a $\ell.o.\ell.$ event under the explicit assumption that each day's load is represented by its daily peak value. In other words, the *LOLE* is evaluated under a worst-case condition: that the daily peak load value persists throughout the 24 hours of each day. As such, the daily peak load representation in the *LOLE* evaluation is unable to capture the more realistic situation that the $\ell.o.\ell.$ event happens only in those hours of day in which the hourly load exceeds the corresponding hourly system total available generation capacity, which are captured by the *LOLH*. Furthermore, the resource adequacy metrics discussed so far do not consider the severity of the $\ell.o.\ell.$ event. A metric that evaluates the sum of the average firm hourly load shed, expressed in MWh, is the *EUE*. The *EUE* metric measures the expected value of energy not served due to inadequate available generation capacity in the system that causes the $\ell.o.\ell.$ events in the period $\mathscr{T}_h$.

To evaluate the resource adequacy metrics for the system with $\underline{\boldsymbol{\kappa}}$ integrated *RR* capacity, we define for each hour h and each simulation run i, the hourly $\ell.o.\ell.$ event binary index

$$\beta^{(i)}[h]\Big|_{\underline{\boldsymbol{\kappa}}} = \begin{cases} 1, & if\ \ell^{(i)}[h]\Big|_{\underline{\boldsymbol{\kappa}}} - a^{(i)}[h] > 0 \\ \\ 0, & otherwise \end{cases} , \tag{4}$$

where $a^{(i)}[h]$ denotes the aggregate available generation capacity in hour h for simulation run i. Therefore, the index returns 1 whenever there is a $\ell.o.\ell.$ event in hour h, otherwise returns zero. We further define the capacity deficiency for each hour h as

$$\delta^{(i)}[h]\Big|_{\underline{\boldsymbol{\kappa}}} = \max\left\{0,\ \ell^{(i)}[h]\Big|_{\underline{\boldsymbol{\kappa}}} - a^{(i)}[h]\right\} . \tag{5}$$

We denote the *LOLP* for the entire period $\mathscr{T}_h$ at a given level of *RR* capacity $\underline{\boldsymbol{\kappa}}$ as $\rho_{\mathscr{T}_h}\Big|_{\underline{\boldsymbol{\kappa}}}$. Then for each simulation run i

$$\rho^{(i)}_{\mathscr{T}_h}\Big|_{\underline{\boldsymbol{\kappa}}} = \sum_{h=1}^{H} \beta^{(i)}[h]\Big|_{\underline{\boldsymbol{\kappa}}} \frac{hours}{H\ hours} . \tag{6}$$

Note that the *LOLP* evaluated for the entire period $\mathscr{T}_h$ under hourly time granularity of the load is equivalent to the *LOLH* metric for the same period. Similarly, the *EUE* can be evaluated by

$$u^{(i)}_{\mathscr{T}_h}\Big|_{\underline{\boldsymbol{\kappa}}} = H \cdot \sum_{h=1}^{H} \delta^{(i)}[h]\Big|_{\underline{\boldsymbol{\kappa}}}\ MWh , \tag{7}$$

where $u^{(i)}_{\mathscr{T}_h}\Big|_{\underline{\boldsymbol{\kappa}}}$ denotes the *EUE* value in the simulation run i, for the period $\mathscr{T}_h$ and at a given level of *RR* capacity $\underline{\boldsymbol{\kappa}}$. To evaluate the *LOLE* metric for the simulation run i, we require the knowledge of how many days in the study period experience a $\ell.o.\ell.$ event. As such, for every day in the period, we need to check whether there exists at least a single hour h in the day with a positive value for the $\beta^{(i)}[h]\Big|_{\underline{\boldsymbol{\kappa}}}$ index. The idea is that if the system available capacity is exceeded by at least one hourly load value, then we are sure that it is also exceeded by the daily peak load, which is used to represent the 24 hours of the day in the *LOLE* evaluation. Hence, the *LOLE* can be evaluated as the expected value of a daily binary index that returns 1 whenever there is a positive value of the hourly index in a single day in the period or otherwise returns 0. After N simulation runs, the final values of all resource adequacy metrics are assessed as the simple average of the sequence of N values, each value generated at the end of every simulation run.

III. Framework Applications

A significant aspect of this paper is the broad range of applications of the proposed framework to study both the short and longer-time periods for planning, operations and other purposes. More specifically, with the proposed framework we perfomed extensive simulation studies, the details of which are given in the following section, to quantify the impacts of deepening *RR* penetrations on the resource adequacy of large-scale grids. For a study period $\mathscr{T}_h$ and at a specified level of installed *RR* capacity $\underline{\boldsymbol{\kappa}}$, we define the generation penetration of the *RR* group q as the ratio of the total generation from *RR*s in the group over the total energy produced by all the system supply resources in the period. We denote the generation penetration of the *RR* group q by γ^q. We further define the vector of *RR* generation penetration for the entire system $\underline{\boldsymbol{\gamma}} \in \mathbb{R}^Q$ as

$$\underline{\boldsymbol{\gamma}} = \left[\gamma^1\ \gamma^2\ \ldots \gamma^Q\right]^\dagger . \tag{8}$$

We emphasize that each γ^q is a function of the installed *RR* capacity κ^q, the system loads and supply/demand resource generation. As such, the values of $\underline{\boldsymbol{\gamma}}$ can be obtained from the realizations of the conventional resource availability and *RR* generation output *r.p.*s. The distinct impacts of the penetrations of each group of *RR*s have not been quantified so far in the way performed in our studies.

The implementation of the proposed framework provides the ability to facilitate the computation of additional metrics required in resource adequacy studies. In this paper, we are particularly interested to study the marginal behavior of the resource adequacy metrics with respect to the deepening *RR*

penetrations. In this regard, we augment the set of metrics with new sensitivity indices with the objective to measure each metric's sensitivity with respect to the penetration γ^q around a reference penetration level $\underline{\boldsymbol{\gamma}}_0$. More specifically, if we assume a small variation $\delta\gamma^q$ for the *RR* group q, then the sensitivity of the resource adequacy metric χ with respect to γ^q is defined as

$$\psi^{\chi}_{\gamma^q}\Big|_{\underline{\boldsymbol{\gamma}}_0} = \frac{\chi\big|_{\underline{\boldsymbol{\gamma}}_0+\underline{\mathbf{1}}^q\delta\gamma^q} - \chi\big|_{\underline{\boldsymbol{\gamma}}_0}}{\delta\gamma^q}, \tag{9}$$

where $\underline{\mathbf{1}}^q = [0, 0, \ldots, 1, \ldots, 0]^\dagger$ with entry 1 in the q^{th} row. The sensitivity index $\psi^{\chi}_{\gamma^q}\Big|_{\underline{\boldsymbol{\gamma}}_0}$ captures the change in the resource adequacy metric χ with respect to γ^q and aims to provide additional insights on how each group of *RR*s may have different influence on the resource adequacy of the system.

Another application of interest of this framework is for the computation of the *ELCC* of each *RR*. More specifically, to obtain the *ELCC* of a particular *RR* unit, multiple applications of the framework can be performed to obtain the resource adequacy metrics with and without the integrated *RR* resource. The *ELCC* of the resource may be evaluated as the additional conventional/controllable generation capacity required to attain the same resource adequacy metric with the *RR* unit integrated into the grid. Furthermore, the framework allows for the evaluation of resource adequacy metrics for data even with different time resolutions.

IV. Representative Case Study Results

Motivated by the recent policy initiatives in California and New York [2], [3] to supply $50\,\%$ of the electricity consumption in each state from *RR*s by 2030, we illustrate the proposed framework with a study of the impacts of such an initiative on the grid resource adequacy. The focus of the application studies reported here is on solar and wind *RR*s, i.e., $Q = 2$. We apply the resource adequacy evaluation framework in a large-scale, representative test system [17] with annual summer peak load forecast for 2030 equal to $36,800\,MW$. Hourly load values from the New York control area (*NYCA*) from the period 2011-2015 are used to construct the *s.p.*s of the system load. The conventional generation resources in the system have a total nameplate capacity of $31,500\,MW$ and include coal, gas, oil and nuclear units. The supply resources also include $6,000\,MW$ of hydro generation. The imports into the system are represented as a constant injection of $2,500\,MW$. We assume no *DRR*s in the system, i.e., all the demand is met by conventional generation units, imports and *RR*s. We model each conventional generation resource as a two-state unit with its own failure/repair rate. The imports are modeled as a conventional generation unit that is $100\,\%$ available — in effect as a reduction of the load by $2,500\,MW$. For the representation of the wind and solar output *s.p.*s, we use 5-year historical wind and solar data from the geographical footprint of *NYCA* for the 2011-2015 period. The 12 wind farms and the seven solar farms are spread at various locations in the *NYCA* footprint. The total nameplate capacities of the integrated wind and solar generation resources are $15,000\,MW$ and $4,000\,MW$, respectively.

To study the effects of the deepening *RR* penetrations on the resource adequacy metrics, we perform two sets of studies on the system. In the first study set, we consider the grid with the integrated solar and wind farms and the existing fleet of conventional resources. We evaluate the *LOLE*, *LOLH* and *EUE* metrics for each specified pair of solar and wind capacity values and compute their associated sensitivities as defined in (9). In the second study set we assess the impacts of the retirement of conventional generation capacity on the resource adequacy metrics. In this study, solar and wind resources are integrated into the grid via the gradual replacement of conventional capacity. Such an implementation provides a more realistic perspective on the effects of deepening *RR* penetrations into the grid's resource adequacy as the integration of *RR*s aims to replace polluting fossil-fired generation resources. The application and sensitivity studies are carried out for a period of 8760 hours for the year 2030.

In the application studies, we construct 59 different cases of integrated solar and wind capacities that correspond to different generation penetrations, i.e., different values of $\underline{\boldsymbol{\gamma}} = [\gamma^s,\ \gamma^w]^\dagger$. In this section we adopt superscript s and w notation to denote the group of solar and wind resources respectively in order to facilitate the discussion of the study results. We define the set of cases $\mathscr{C} = \{c_j : j = 1, \ldots, 59\}$ where each case c_j is represented by the capacity vector $\underline{\boldsymbol{\kappa}}_j = \left[\kappa^s_j,\ \kappa^w_j\right]^\dagger$, which corresponds to the penetration vector $\underline{\boldsymbol{\gamma}}_j = \left[\gamma^s_j,\ \gamma^w_j\right]^\dagger$. Clearly, $\underline{\boldsymbol{\kappa}}_1 = [0,\ 0]^\dagger$ results in $\underline{\boldsymbol{\gamma}}_1 = [0,\ 0]^\dagger$, i.e., the system has zero generation penetrations of solar and wind resources in the case c_1. The study case c_{59} corresponds to $\underline{\boldsymbol{\kappa}}_{59} = [4,000,\ 15,000]^\dagger$ and gives $\underline{\boldsymbol{\gamma}}_{59} = [6.03\ 20.06]^\dagger$, i.e., the maximum total generation penetration of solar and wind obtained is 26.09%. The study system has a 25% penetration from renewable hydro generation and as such, to achieve the goal of 50% total penetration from *RR*s, we need an additional 25% from wind and solar resources. Therefore, the goal of 50% *RR* penetration is achieved for the study system in case c_{59}.

We construct the 59 cases by the combination of nine values for κ^s_j and 13 values for κ^w_j. For the solar capacity, κ^s_j takes values from $0\,MW$ to $4,000\,MW$ with increments of $500\,MW$. The wind installed capacity, κ^w_j takes values from $0\,MW$ to $15,000\,MW$ with increments of $1,250\,MW$. We do not consider every possible combination (9×13) of κ^s_j and κ^w_j, but rather limit the framework applications to a subset of combinations that are representative and sufficient to derive meaningful results. For each case, the system has a specific value of total installed solar and wind capacity denoted by κ^s_j and κ^w_j respectively.

To evaluate the metric sensitivities under the retirement of conventional capacity we introduce the notion of a retirement factor denoted by ζ. We define ζ as the fraction of the retired conventional capacity of the total solar and wind capacity

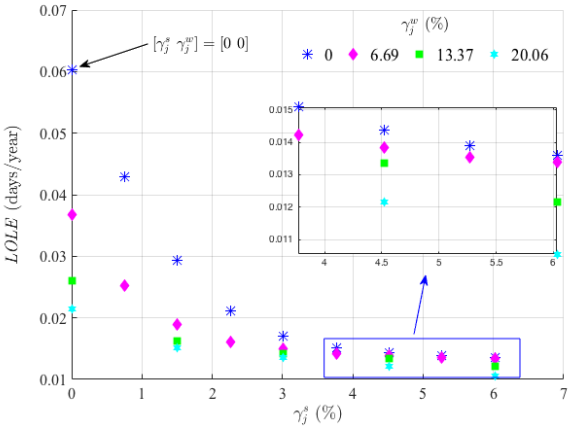

Fig. 2. *LOLE* values for different wind and solar penetrations.

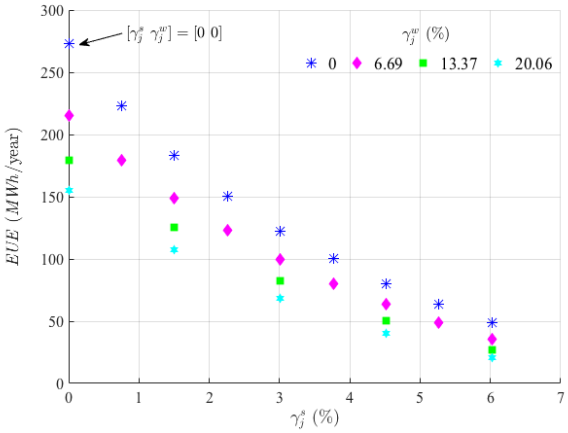

Fig. 4. *EUE* values for different wind and solar penetrations.

added. We carry out simulation studies with the retirement factor ζ assuming the values in the set

$$\mathscr{Z} = \{\zeta_i = 0.05i, i = 1, 2, ..., 18\} \ . \tag{10}$$

For example, $\zeta_2 = 0.1$ implies that for $100\,MW$ of nameplate solar and wind capacity integrated in the system, $10\,MW$ of conventional capacity is retired. We construct a total of 373 cases from a subset of cases $c_j \in \mathscr{C}$ and for each $\zeta_i \in \mathscr{Z}$ and evaluate the resource adequacy metrics. Note that the resulting solar and wind penetrations in each case depend both on the values of the installed wind and solar capacities but also on the values of ζ_i.

We start out with a discussion of the key results and findings for the first set of studies without the combination of retirements in the resource mix. In Figs. 2–4 we plot the *LOLE*, the *LOLH* and the *EUE* metric for deepening wind and solar penetrations. Each point in the diagrams represents a different case, which corresponds to a distinct pair of values $\left[\gamma_j^s, \gamma_j^w\right]^\dagger$. The study results indicate that each metric decreases as the penetrations of wind and/or solar generation increase. For example, the *LOLE* for case c_1 is equal to 0.06 days/year and it drops to approximately 0.01 days/year for case c_{59} ($[\gamma_{59}^s\ \gamma_{59}^w]^\dagger = [6.03,\ 20.06]^\dagger$). If the study system were to comply to the *LOLE* ≤ 0.1 days/year criterion (or "1 day in 10 years"), then the system is resource adequate even in the case c_1. Thus the installed conventional generation resource capacity and the imports from neighboring entities suffice to meet the system's total forecasted load in 2030 without any integrated wind/solar resources. Similar decline with the *LOLE* is observed on both the *LOLH* and *EUE* metrics. For example, the *LOLH* index drops from 0.182 hours/year to 0.025 hours/year for cases c_1 and c_{59} respectively. The corresponding values for the *EUE* are $273.0\,MWh$/year which drops to only $20.805\,MWh$/year. The decline in the resource adequacy indices is certainly not surprising given the $19,000\,MW$ of added *RR* capacity for case c_{59}. However, we note that the decline in the metrics is diminishing as the penetrations of wind and solar deepen. Indeed, the scatter "curves" become flatter (less sloped) as we move towards the right. The behavior of the metrics indicates diminishing marginal returns, which is also verified from the sensitivities of each metric. In Figs. 5 and 6 we present the *LOLE* sensitivity indices with respect to solar and wind penetrations. The complete results for all the metric values and sensitivities for each case considered can be found in [17]. From these diagrams we observe that the sensitivity of the *LOLE* decreases as the penetrations of wind and solar generation increase. The results indicate that the reduction in the *LOLE* becomes smaller as we deepen the *RR* penetrations into the grid. For example, from Fig. 6 we note that for $\gamma_j^s = 0$, an increase of γ_1^w from $0\,\%$ to γ_2^w at $1.67\,\%$ results in a decrease of the *LOLE* of approximately 45.69×10^{-4} days/year/% of penetration. However, a change from $\gamma_9^w = 13.37\,\%$ to $\gamma_{10}^w = 16.73\,\%$ results in the reduction of the *LOLE* by only 8.05×10^{-4} days/year/% of penetration. Another interesting observation is that for only 4.52% solar penetration, the decrease in the *LOLE* is slightly greater than zero for a change of wind penetration from 3.35% to as high as 16%. By comparing the results in Figs. 5 and 6 we observe that for this test system, the sensitivities under deepening solar

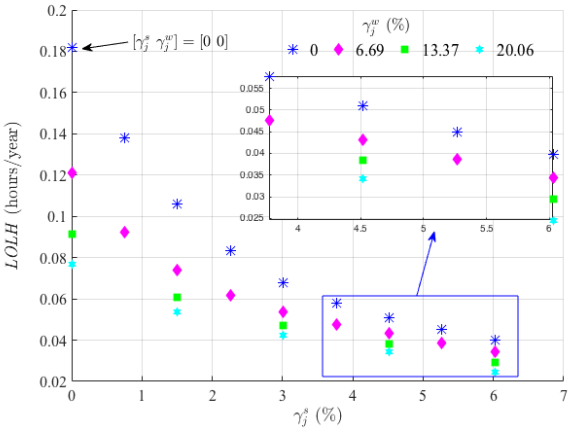

Fig. 3. *LOLH* values for different wind and solar penetrations.

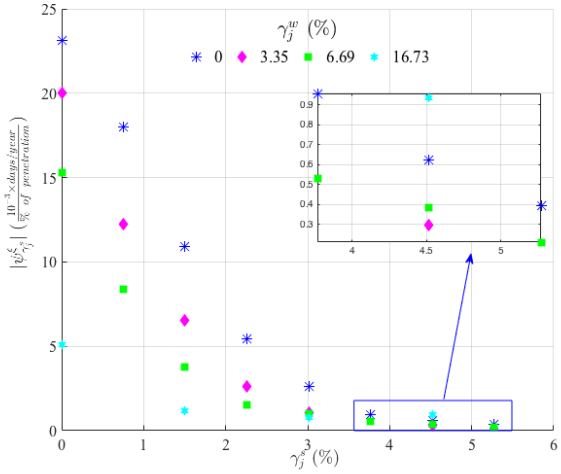

Fig. 5. Sensitivity of the *LOLE* metric with respect to solar generation penetration.

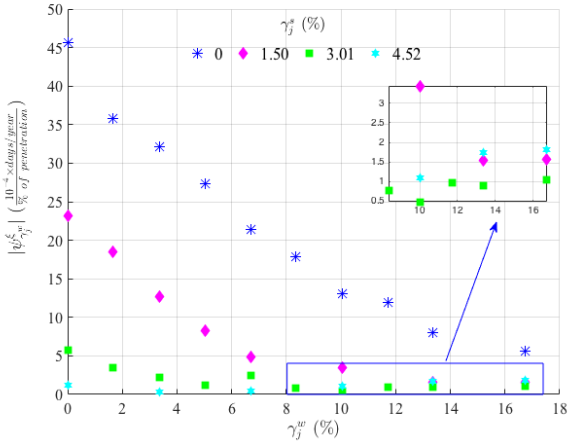

Fig. 6. Sensitivity of the *LOLE* metric with respect to wind generation penetration.

and wind penetrations are 10 times more impactful for each % change in solar penetration than in wind. Although the deepest solar generation penetration is less than a third of the deepest wind penetration in these application studies, solar appears to be a far more impactful choice than wind to improve the resource adequacy of the system. Such results make sense because of the generally good and consistent tracking of the load by the solar generation during the peak summer months. In fact, the hot summer days, when the load is close to or reaches its peak value, are the days or hours of day with the highest contribution to the *LOLE*. Therefore, the solar resources integrated into such systems, contribute significantly more to reduce the *LOLE* metric than wind as a function of the penetration level. On the other hand, the mismatch of the wind generation with the load is so consistent, that an approximately four times greater capacity addition of wind has an order of magnitude smaller impact on the *LOLE*.

In the second set of studies we evaluate the resource adequacy metrics with respect to γ_j^s, γ_j^w and ζ_i. For each value of ζ_i we require that the system satisfies the "1 day in 10 years" resource adequacy criterion, i.e., $LOLE \leq 0.1$ days/year. Therefore, any combination of values of $\underline{\gamma}_j$ and ζ_i that results in $LOLE > 0.1$ days/year, is assumed to make the system inadequate to supply its forecasted load in 2030. In Figs. from 7 to 10 we plot the *LOLE* metric for different values of ζ_i and *RR* penetrations. The abscissa (ordinate) in the diagrams represents solar (wind) generation penetrations. The center of each circle in the diagrams corresponds to a distinct pair of $\left[\gamma_j^s, \gamma_j^w\right]^\dagger$ for a specified value of ζ_i. The size of each circle represents the value of the *LOLE* metric. Our focus is not at the exact value of the *LOLE* at each case but rather wish to investigate how the solar and wind penetrations affect the *LOLE* at a specified conventional resource retirement factor. Each circle in Fig. 7 depicts the *LOLE* value that results under $\zeta_2 = 0.1$, i.e., for every $10\,MW$ of integrated solar and wind generation capacity, $1\,MW$ of conventional generation capacity is removed from the system. For example, the circle with center $[0, 28.4]^\dagger$ corresponds to the system with $0\,MW$ integrated solar capacity and $15,000\,MW$ of integrated wind capacity. The retirement factor $\zeta_2 = 0.1$ allows the retirement of $1,500\,MW$ conventional capacity. The plot indicates that for $\zeta_2 = 0.1$ the *LOLE* values decrease with increasing solar and wind penetrations, although the decrease is more marked for solar penetrations. Our

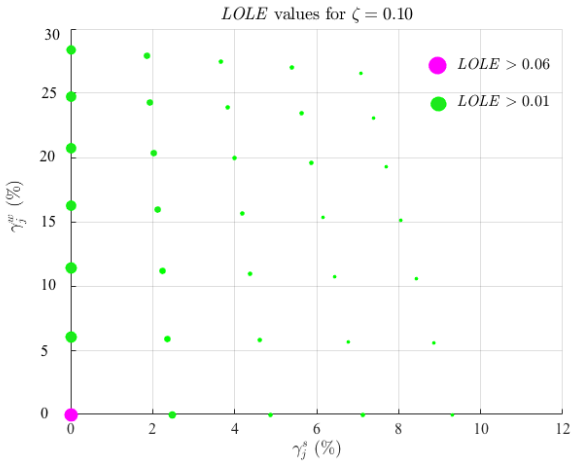

Fig. 7. *LOLE* metric for 10% conventional generation retirement.

simulation studies further indicate that the decrease in the *LOLE* values for deeper wind penetrations, seizes to occur for $\zeta_i \geq 0.25$. Conventional capacity retirement factors of 0.25 (0.5) means that for every $10\,MW$ of integrated *RR* capacity, $2.5\,MW$ ($5\,MW$) of conventional capacity is retired. In these cases, the substitutability of retired generation by wind resources becomes so limited that the addition of multiples of the retired conventional capacity by wind resources is inadequate to maintain the "1 day in 10 years" criterion. We point out, however, that solar substitutability continues to be considerable at both $\zeta_5 = 0.25$ and $\zeta_{10} = 0.50$ retirement

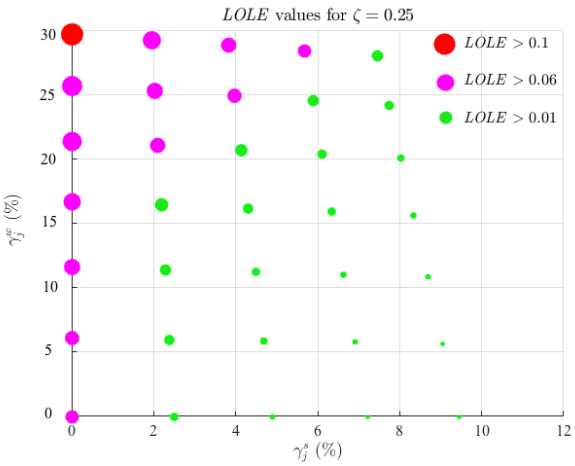

Fig. 8. *LOLE* metric for 25% conventional generation retirement.

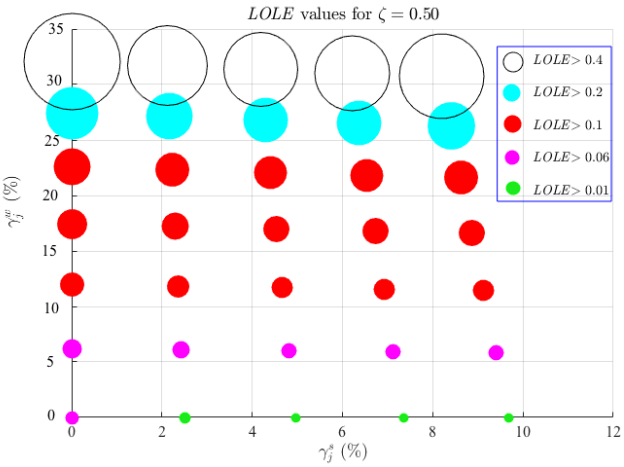

Fig. 9. *LOLE* metric for 50% conventional generation retirement.

factors. Such outcomes that highlight the distinct behavior of wind and solar resources, are induced by the tracking ability of solar during the peak summer months and the marked anti-correlated behavior of wind resources with the load.

The tracking ability of solar resources during the peak summer months is limited for $\zeta_i \geq 0.5$. Indeed, as illustrated in Fig. 10 the *LOLE* metric increases rapidly with both solar and wind generation penetrations. We note that for $\zeta_{18} = 0.9$, although we start with a resource adequate system that satisfies *LOLE* < 0.1 days/year, we end up with *LOLE* > 2 days/year. More specifically, at $19,000\,MW$ of total installed wind and solar capacity and $17,100\,MW$ retired conventional capacity, the *LOLE* $\backsimeq 6.0$ days/year — an unacceptably high value. Such limitations on *RR* substitutability for retired conventional capacity require careful attention from grid operators. The approach used in the studies makes effective use of the framework to facilitate the development of appropriate retirement schedules that have acceptable resource adequacy characteristics.

V. Conclusions

The marked cost reductions in renewable technology are key drivers in the wider implementation of *RR*s everywhere. This paper focuses on the critical aspect of resource adequacy and on the quantification of the impacts of deepening *RR* penetrations in the grid's reliability. The limitations of the time-abstracted framework in the incorporation of the intermittent and time-varying nature of *RR*s motivated the development of a simulation-based, time-dependent resource adequacy framework with the capability to represent the uncertain and time-varying nature of loads and demand/supply resources, including the intermittency in the outputs of *RR*s. The framework provides additional degrees of freedom for the definition and evaluation of new resource adequacy metrics that are particularly appropriate for the study at hand. As such, we develop new sensitivity indices to quantify the marginal behavior of each resource adequacy metric with respect to the deepening *RR* penetrations.

The effectiveness of the time-dependent framework is demonstrated via its extensive applications to evaluate the resource adequacy of large-scale study systems. In the studies, we characterize the impacts of deepening *RR* penetrations on the resource adequacy through the behavior of the evaluated metrics — *LOLH*, *LOLE* and *EUE*. The study results demonstrate the improvement in the grid resource adequacy — indicated by the declining values of the metrics — as the penetrations of wind and solar resources deepen. Furthermore, solar resources appear to have a significantly more pronounced impact on the metrics than wind, as the better tracking of the load by solar generation during the peak summer months is consistent with the summer peaking study system. Another important finding is the diminishing marginal returns characteristic on each metric associated with the deepening wind and solar penetrations. However, the tracking ability of solar is insufficient to replace the increase in the retired conventional generation capacity. In fact, the resource adequacy of the study system begins to deteriorate, i.e., the values of the adequacy metrics increase with the conventional generation retirement. Notwithstanding the deepening *RR* penetrations, when the retirement factor exceeds 0.25, the inability of the grid to meet the "1 day in 10 years" criterion becomes evident. Such limitations of *RR*s in the provision of resource adequacy, can impact the retirement schedule of fossil-fired units. The resource adequacy issue in electric power grids becomes significant given the push to displace the outputs of polluting fossil-fired generation resources and the imminent retirement of many such units.

References

[1] European Cmmission, "Directive of the European Parliament and of the Council: On the Promotion of the Use of Energy from Renewable Resources (recast)," November 2016. [Online]. Available: https://ec.europa.eu/energy/sites/ener/files/documents/1_en_act_part1_v7_1.pdf

[2] California Energy Cmmission, "Clean Energy and Pollution Reduction Act of 2015," August 2016. [Online]. Available: https://leginfo.legislature.ca.gov/faces/billNavClient.xhtml?bill-id=201520160SB350

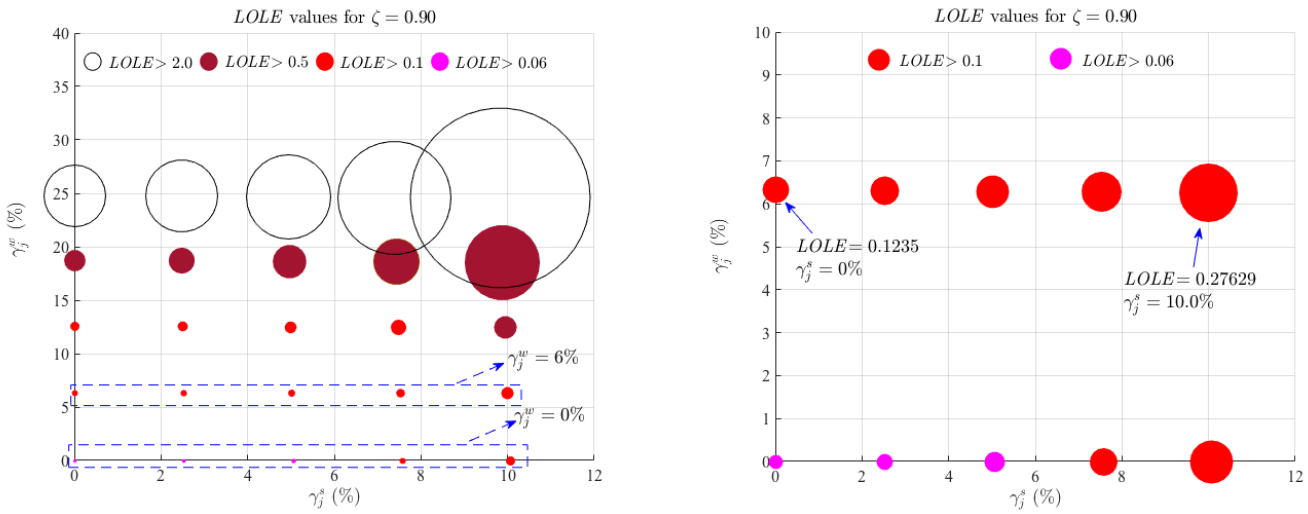

(a) $0\% \leq \gamma_j^w \leq 25\%$

(b) $\gamma_j^w = 0\%$ and $\gamma_j^w = 6\%$

Fig. 10. *LOLE* metric for 0.9 retirement factor.

[3] State of New York Public Service Cmmission, "Order Adopting a Clean Energy Standard," August 2016. [Online]. Available: http://documents.dps.ny.gov/public/MatterManagement/CaseMaster.aspx?MatterCaseNo=15-e-0302

[4] North American Electric Reliability Corporation, "Glossary of Terms Used in NERC Reliability Standards," August 2016. [Online]. Available: http://www.nerc.com/files/glossary_of_terms.pdf

[5] J. Zhang and A. Dominguez-Garcia, "Evaluation of Demand Response Resource Aggregation System Capacity Under Uncertainty," *IEEE Transactions on Smart Grid*, vol. PP, no. 99, pp. 1–1, 2017.

[6] J. Endrenyi, *Reliability Modeling in Power Systems*. Toronto, Canada: John Wiley and Sons, 1978.

[7] IEEE Power and Energy Society, "IEEE Standard Definitions for Use in Reporting Electric Generating Unit Reliability, Availability, and Productivity," March 2007. [Online]. Available: http://www.nerc.com/docs/pc/gadstf/ieee762tf/762-2006.pdf

[8] C. D'Annunzio and S. Santoso, "Noniterative Method to Approximate the Effective Load Carrying Capability of a Wind Plant," *IEEE Transactions on Energy Conversion*, vol. 23, no. 2, pp. 544–550, June 2008.

[9] N. Maisonneuve and G. Gross, "A Production Simulation Tool for Systems With Integrated Wind Energy Resources," *IEEE Transactions on Power Systems*, vol. 26, no. 4, pp. 2285–2292, Nov 2011.

[10] North American Electric Reliability Corporation, "Methods to Model and Calculate Capacity Contributions of Variable Generation for Resource Adequacy Planning," March 2011. [Online]. Available: http://www.nerc.com/files/ivgtf1-2.pdf

[11] B. Hasche, A. Keane, and M. O'Malley, "Capacity Value of Wind Power, Calculation, and Data Requirements: the Irish Power System Case," *IEEE Transactions on Power Systems*, vol. 26, no. 1, pp. 420–430, Feb 2011.

[12] L. L. Garver, "Effective Load Carrying Capability of Generating Units," *IEEE Transactions on Power Apparatus and Systems*, vol. PAS-85, no. 8, pp. 910–919, Aug 1966.

[13] R. Duignan, C. J. Dent, A. Mills, N. Samaan, M. Milligan, A. Keane, and M. O'Malley, "Capacity Value of Solar Power," *in Proc. of 2012 IEEE Power and Energy Society General Meeting*, pp. 1–6, July 2012.

[14] R. Billinton and W. Li, *Reliability Assessment in Electric Power Systems Using Monte Carlo Methods*. New York: Springer Science & Business Media, 1994.

[15] Y. Degeilh, "Stochastic simulation of power systems with integrated renewable and utility-scale storage resources," Ph.D. dissertation, Univ. of Illinois at Urbana-Champaign, Urbana, March 2015. [Online]. Available: http://gross.ece.illinois.edu/files/2015/03/Yannick-Degeilh.pdf

[16] J. Kleijnen, *Statistical Techniques in Simulation - Part 1 and 2*. New York: Marcel Dekker Inc., 1974.

[17] M. Ndrio, "Resource adequacy in grids with resources," Master's thesis, Univ. of Illinois at Urbana-Champaign, Urbana, May 2017.

[18] G. Gross, "Notes for ECE 588-Electricity Resource Planning," *Univ. of Illinois at Urbana-Champaign*, Fall 2016.